nature portfolio

Peer Review File

A topological Hund nodal line antiferromagnet

REVIEWER COMMENTS

Reviewer #1 (Remarks to the Author):

The authors, Hasan et al., extensively discuss ARPES data and theoretical modeling of the electronic structure of YMn2Ge2. They assert that the antiferromagnetic ordering in the material leads to symmetry-protected degeneracies of electronic states at the Brillouin zone boundary. On the surface of a finite crystal, these bands reconnect, identified as a drumhead surface state. YMn2Ge2, in general, exhibits strong correlation effects and Hund coupling. Consequently, the spectroscopic signatures are expected to resemble a Hund nodal line phase, as discussed in the literature.

Identifying and preparing a corresponding sample for high-precision ARPES spectroscopy is a challenging task, as outlined comprehensively and technically by the authors. I appreciate the openness in addressing discrepancies in the theoretical modeling of the same material.

However, at the current stage, I don't find the paper suitable for publication in a high-impact journal like Nature Communications. I would like to express my concerns below for discussion by the authors.

i) The agreement between theoretical band structure calculations and experimental ARPES data is not readily apparent. Comparing, for instance, Fig 1 e,g,i with Fig 1 f,h,j requires a considerable degree of imagination. If there is indeed agreement, it would be beneficial to superimpose the calculated band structure on the measured ARPES spectrum. If there is no agreement, there may be an issue on the theory side that needs correction. The authors use state-of-the-art theoretical tools, which should be capable of sufficiently reproducing the ARPES data. On the experimental side, is there a method to ensure a well-ordered AFM state and not a superposition of domains, which might complicate agreement with theory?

ii) The "drumhead surface state" is highly dispersive. Although the authors show localization at the surface (Fig 4a), it does not necessarily confirm it as an actual surface state. The authors mention they have constructed a tight-binding model to verify this behavior. Some clarification: On the tight-binding level, surface states typically exhibit a strong decay of wave functions weights, moving from sites at the surface layer into the bulk. In contrast, bulk states show a sine-function behavior. However, in "magnetic topological materials," wave functions can display a cosine behavior, i.e., a strong contribution at the surface but oscillatory behavior in the bulk. A plot along a few selected points of the drumhead could serve as a good proof.

iii) Personally, I find the manuscript's text to be somewhat overselling. Firstly, topology is not a new topic in condensed matter physics, and repeatedly listing existing examples can be tiresome. The motivation for adding yet another example is valid but could be published in a more specialized journal. Additionally, strictly speaking, the authors discuss an antiferromagnetic metal with degeneracies in the band structure. The same applies to "Hundness." I don't believe that Hund coupling and the interplay of strong correlations and magnetism are novel concepts that need verification.

iv) While the authors cite a somewhat random collection of more or less related topological states, a stronger focus on prior work in the area of electronic states in the presence of Hund coupling is recommended (e.g., Alonso et al., Phys. Rev. B 64, 054408, 2021). Specifically, referring to previous work on "Hund nodal lines," such as Geilhufe, Guinea, Juricic, Phys. Rev. B 99, 020404(R), 2019, would improve the manuscript's coherence.

R. Matthias Geilhufe, Chalmers University of Technology

Reviewer #2 (Remarks to the Author):

The paper by Xian P. Yang et al. presents the electron structure of antiferromagnet YMn2Ge2 measured with ARPES. Compared with DFT and DMFT calculations, the authors suggest the fourfold degenerate Dirac nodal line states remain at the boundary of the bulk Brillouin zone ZRA plane, which is protected by PT symmetry and nonsymmetric lattice symmetry. Furthermore, the authors compare the band d-orbital dependent renormalization factors from DFT, DMFT, and experiment results, and they claim that this Dirac nodal line is due to Hund's coupling so that this Dirac nodal line is a magnetic topological phase under electron correlations.

The paper is clear, and the findings are important for the topological and correlated matter community. I believe it's the first direct experiment result that observed the AFM Dirac nodal line states and the experiment measurements agree well with the theoretic band structures, which fill a gap in the magnetic topological materials.

Apart from the advantages of this work, I have the following concerns and comments that need to be addressed prior to a recommendation for publication.

1. My main concern is that the bulk band crossing has not been fully proven to be bulk bands. On the contrary, they look more likely to be surface states in Fig. 2. I agree the Fermi surface mapping in Fig. 1c and Fig. 2a agree well with the DFT results, but the DFT results are dominated by surface states. How do the authors argue the crossing bands are bulk Dirac nodal states? In addition, in Fig. 4a, the DFT results show a crossing surface state close to the DP, so the pure surface states can also form the band shape in Fig. 1g. Extended Figs. 2 and 3 support the band along cut1 are bulk

bands and they have crossing point along A-M, but the crossing points are very broad, which is hard to support the nodal line band structure. Additional evidence is necessary to prove the band along cut2 is a real bulk band crossing.

2. How can we understand the drumhead surface states and why are the surface states split into two? Do they have different spin components? The authors should elaborate more on these drumhead surface states, e.g., are they different from non-magnetic Dirac nodal line drumhead surface states?

3. The bands maintain the fourfold degenerate along the M-A Brillouin boundary shown in Extended Figs. Are they also the Dirac nodal line?

4. The band crossing along A-Z looks like parabolic lines. Could this crossing be proven as linear dispersion theoretically?

5. The DFT results in Fig. 1d, f, h, j should be drawn in the same region as the experiment for better comparison.

6. The axis region in Fig. 1i looks strange; the cut1 is -1 to 1, but the x-axis of Fig. 1i is 0 to 2, and the ARPES result in Fig. 1i looks like 0.5 to -1.5.

7. The region and high symmetry points of the 2nd Brillouin zone in Fig. 2a need to be added for clarity.

Reviewer #3 (Remarks to the Author):

The manuscript of X. P. Yang et. al. „A Hund nodal line antiferromagnet“ reports Dirac nodal line along at the boundary of bulk Brillouin zone and a drumhead surface states through the whole surface Brillouin zone in YMn2Ge2 antiferromagnet. Electron correlation effects are unveiled.

The topic and material in general are interesting and important for the state of the art research. The nodal line looks confirmed, the results of the first manuscript half presented clear.

But with the drumhead surface state in this research there are problems. I do not see it on experimental data. The black dashed line at Fig. 4b goes differently from calculation at Fig. 4a. At Fig. 4a it initially coincides with the bulk state, at Fig. 4b goes initially apart from the bulk state. The surface state and bulk state do not coincide at the zone border at X at Fig. 4a. Extended Fig. 5 shows a different picture inside the zoom-in green box compared to the left panel. I expect also that the drumhead surface state should be visible at Fig. 2, but it is not visible. Why? The calculation of Fig. 4a shows a huge number of surface bands. By which criteria some of the bands are considered and others neglected in the discussion? With such number of calculated surface bands one can find anything and a faint band on one of the measurements (but not others) can be attributed also to anything.

As the result, an important part of the manuscript is unconfirmed within the current presentation and can not be published in the present form.

Authors' Reply to Referees' Comments

We wish to thank all Referees for their insightful comments and suggestions, which greatly helped improve our manuscript. In the following, we carefully address their comments.

Reviewer #1 (Remarks to the Author):

The authors, Hasan et al., extensively discuss ARPES data and theoretical modeling of the electronic structure of YMn2Ge2. They assert that the antiferromagnetic ordering in the material leads to symmetry-protected degeneracies of electronic states at the Brillouin zone boundary. On the surface of a finite crystal, these bands reconnect, identified as a drumhead surface state. YMn2Ge2, in general, exhibits strong correlation effects and Hund coupling. Consequently, the spectroscopic signatures are expected to resemble a Hund nodal line phase, as discussed in the literature.

Identifying and preparing a corresponding sample for high-precision ARPES spectroscopy is a challenging task, as outlined comprehensively and technically by the authors. I appreciate the openness in addressing discrepancies in the theoretical modeling of the same material.

However, at the current stage, I don't find the paper suitable for publication in a high-impact journal like Nature Communications. I would like to express my concerns below for discussion by the authors.

We would like to sincerely thank the Referee for the detailed comments and questions, and we will respond to these comments below.

i) The agreement between theoretical band structure calculations and experimental ARPES data is not readily apparent. Comparing, for instance, Fig 1 e,g,i with Fig 1 f,h,j requires a considerable degree of imagination. If there is indeed agreement, it would be beneficial to superimpose the calculated band structure on the measured ARPES spectrum. If there is no agreement, there may be an issue on the theory side that needs correction. The authors use state-of-the-art theoretical tools, which should be capable of sufficiently reproducing the ARPES data. On the experimental side, is there a method to ensure a well-ordered AFM state and not a superposition of domains, which might complicate agreement with theory?

We thank the Referee for the comment. One of our main conclusions in this study is that the magnetic nodal line in YMn_2Ge_2 is strongly renormalized due to Hund's coupling. As shown in Fig. 1j, A and R points consist of mostly d_{z^2} and d_{xy} orbitals, respectively. Therefore, distinct renormalization factors are needed for both d orbitals (or bands near A and R points), as an essential signature of a Hund's metal (Fig. 3). As a result, our globally renormalized DFT in Fig. 1 can only qualitatively catch the main features in the band structure, namely the energy position of the nodal point at R in Figs. 1g-h and the shape of the fourfold degenerate nodal line in Figs. 1i-j. At the same time, band dispersions at A point in DFT calculations deviate from ARPES data in Figs. 1e-f. The fact that DFT calculations don't fully agree with ARPES data near the Fermi level motivates us to apply DFT+DMFT to understand the band dispersion and electronic correlations. The important role Hund's coupling plays in this material is exactly the point we would like to emphasize in the manuscript.

To make it clearer to readers, we modify our text: "It is intriguing to note that to better match ARPES data, all bulk electronic bands in DFT calculations are renormalized by a factor of 3, suggesting the presence of strong electronic correlations in YMn_2Ge_2. Despite the overall good agreement especially the energy position of the nodal point at the R point in Figs. 1**g-j** and the shape of the nodal line in Figs. 1**i-j**, the binding energy position of the Dirac crossing at the A point differs from renormalized DFT calculations, as shown by the red dashed line in Figs. 1**e-f**. Instead, a smaller renormalization factor (less than 3) should be applied at the A point so that the bands are less "compressed" below the Fermi level. As we will show later, this magnetic nodal line manifests a strong *d* orbital dependent renormalization due to Hund's coupling. Therefore, DFT results in Fig. 1 don't fully agree with ARPES data, indicating the necessity of DFT + DMFT calculations that will improve the agreement (Supplementary Fig. 4 and Fig. 3)."

Furthermore, we add a new figure as Supplementary Fig. 4, which superimposes the DFT and the corresponding DFT+DMFT results on ARPES data (cuts 2 and 3 in Fig. 1) to highlight our argument. In Supplementary Fig. 4a, the Dirac dispersion in DFT matches well with ARPES data (black arrows), and the bulk band in ARPES near the Z point indicated by the blue arrows is also captured by DFT. The remaining two bands in ARPES near Z point are surface drumhead states (discussed in Fig. 4) so are not revealed in the bulk band DFT calculations. In the corresponding DFT+DMFT, these features remain, as demonstrated by black and blue arrows in Supplementary Fig. 4b. As a comparison, globally renormalized DFT cannot fully capture the band dispersion near the Fermi level along the A-R direction in Supplementary Fig. 4c, since the binding energy of the band near the A point in ARPES deviates from DFT calculations (marked by the black arrow). However, DFT+DMFT calculations with Hund's coupling included instead perfectly agree with ARPES (Supplementary Fig. 4d). Specifically, the dispersion near the A point is well captured by DFT+DMFT results.

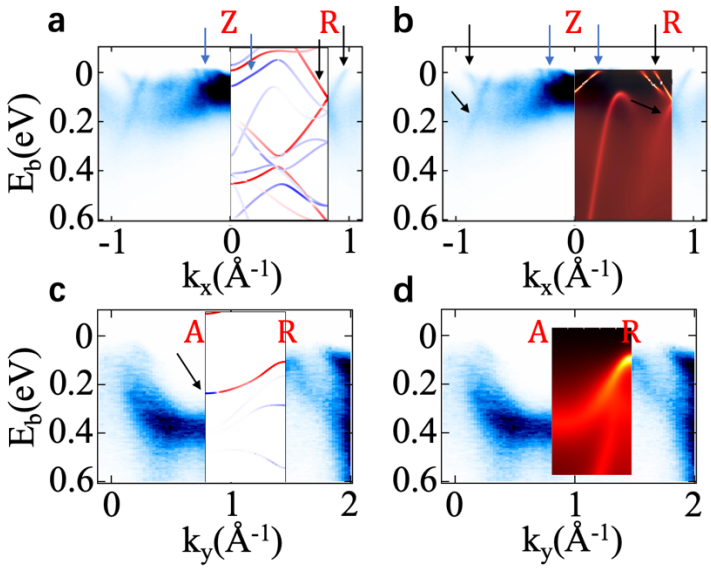

Supplementary Fig. 4. Comparison between ARPES and calculations. a, ARPES dispersion along Z-R direction. Same as Fig. 1**g** or cut 2 in Fig. 1. DFT calculations are superimposed on ARPES to illustrate the overall agreement. Blue and black arrows mark the bulk state at the center of the BZ and the Dirac cone, respectively. **b,** Same as **a,**

except that DFT+DMFT results are superimposed on ARPES data. **c,** ARPES dispersion along A-R direction. Same as Fig. 1**i** or cut 3 in Fig. 1. The embedded DFT calculations deviate from ARPES data, especially near the A point (black arrow). **d,** Same as **c,** except that DFT+DMFT results are superimposed on ARPES data. The inclusion of Hund's coupling improves the agreement with ARPES.

For the comparison above, we only focus on band dispersions near the Fermi level, and we would like to explain the reason below. Given that YMn_2Ge_2 is a Hund metal, the broadening of the spectral function is a distinct feature of the strong correlations. Our DMFT spectral function in Fig. 3 shows the broadening of the spectral function at higher binding energies. For example, the sharp nodal line at R point becomes incoherent at A point. In APRES this Hund nodal line also reveals the same feature. Thus, bands at deeper binding energies are blurred/smeared out in experiments.

Regarding the AFM domain, the ARPES beam spot size is about 10 μm by 30 μm. Since Mn spins point along c axis (Fig. 1a) and the cleaved (001) surface is perpendicular to c axis, we don't need to worry about AFM domains in our experiment. Similar to what previous studies on other AFM materials demonstrate [R1], if the magnetic moment points along a or b axis, the fourfold rotational symmetry of the Fermi surface in Fig. 1d will be broken, which is not what we observe here. Thus, we believe that AFM domain won't complicate our conclusion, as our samples should only have one AFM domain where Mn spins point along c axis.

[R1] Kushnirenko, Y. et al. Directional effects of antiferromagnetic ordering on the electronic structure in NdSb. *Phys. Rev. B* **108**, 115102 (2023).

ii) The "drumhead surface state" is highly dispersive. Although the authors show localization at the surface (Fig 4a), it does not necessarily confirm it as an actual surface state. The authors mention they have constructed a tight-binding model to verify this behavior. Some clarification: On the tight-binding level, surface states typically exhibit a strong decay of wave functions weights, moving from sites at the surface layer into the bulk. In contrast, bulk states show a sine-function behavior. However, in "magnetic topological materials," wave functions can display a cosine behavior, i.e., a strong contribution at the surface but oscillatory behavior in the bulk. A plot along a few selected points of the drumhead could serve as a good proof.

We thank the reviewer for pointing this out. We now confirm theoretically the surface nature of the drumhead state with two pieces of evidence. First, as shown in Supplementary Fig. 12, the two drumhead states only appear in the right panel, which represents the spectral weight of the surface state. As a comparison, they are not in the left panel with only projected bulk states. Second, we calculate the real space charge density distribution of several selected points along the drumhead state in Supplementary Fig. 13. Specifically, points 1 to 4 are along the drumhead state and they are localized at the surface. As a comparison, the charge density of bulk states for points 5 and 6 shows an oscillatory behavior inside the bulk. Thus, the drumhead surface state has a surface origin.

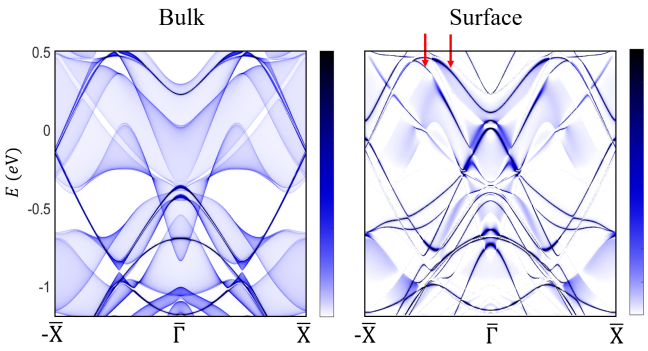

Supplementary Fig. 12. Semi-infinite surface calculations along the $\bar{X}$-$\bar{\Gamma}$-$\bar{X}$ high symmetry direction. Semi-infinite surface calculations excluding (left) and including (right) surface states along the $\bar{X}$-$\bar{\Gamma}$-$\bar{X}$ high symmetry direction. Red arrows mark the two drumhead surface states that only appear in the right panel.

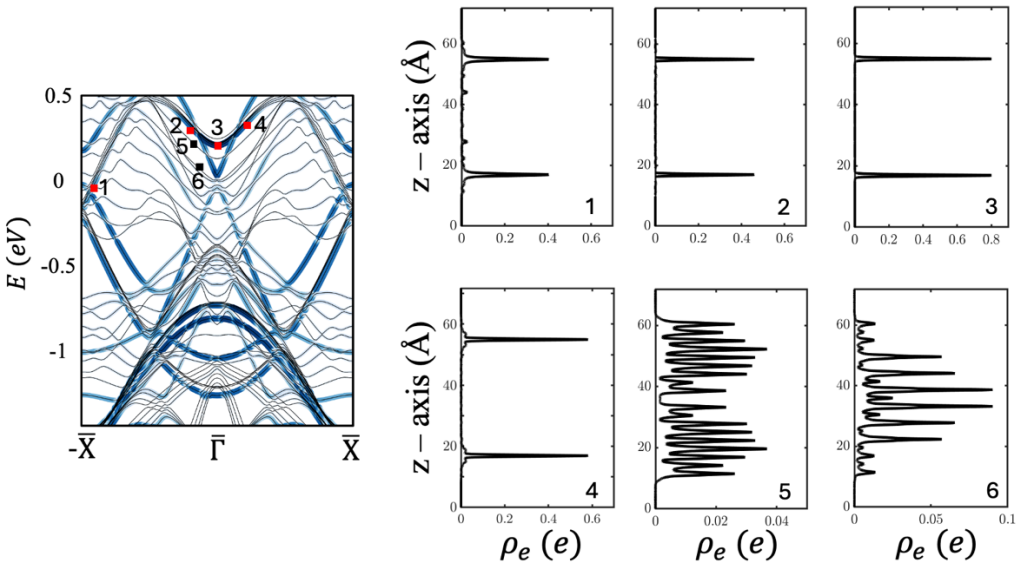

Supplementary Fig. 13. Charge density of selected points along the drumhead surface state and bulk states. **Left**: Finite-size slab calculations along the $\bar{X}$-$\bar{\Gamma}$-$\bar{X}$ high symmetry direction. Blue lines represent the intensity of surface states. Six points are selected. Points 1 to 4 are along the drumhead surface state and 5 to 6 are along bulk states. **Right**: Charge density of the points marked by the red and black squares in the left panel. Based on the charge density of points 1 to 4, the drumhead state is shown to be localized at the surface. As a comparison, the charge density of bulk states for points 5 and 6 shows an oscillatory behavior inside the bulk. Thus, the drumhead surface state has a surface origin.

In addition to our new DFT calculations, we also conduct photon energy dependence of the drumhead state to experimentally verify its surface nature in Supplementary Fig. 9. Thus, the combined DFT and ARPES results should convincingly prove the drumhead states as surface states.

iii) Personally, I find the manuscript's text to be somewhat overselling. Firstly, topology is not a new topic in condensed matter physics, and repeatedly listing existing examples can be tiresome. The motivation for adding yet another example is valid but could be published in a more specialized journal. Additionally, strictly speaking, the authors discuss an antiferromagnetic metal with degeneracies in the band structure. The same applies to "Hundness."

I don't believe that Hund coupling and the interplay of strong correlations and magnetism are novel concepts that need verification.

We thank the Referee for the comment. We modified the text accordingly based on the Referee's comment. Specifically, we shortened our discussions about existing topological materials by removing the lists of topological materials in the introduction and conclusion sections.

Although topology in general is not a new topic in condensed matter physics, like what the second Referee summarizes, our work provides the "*first direct experimental result that observed the AFM Dirac nodal line states*". Combining AFM, spin-orbit coupling, and topology in one system is still quite rare, especially in real materials. For example, 3D AFM Dirac semimetal CuMnAs (*Nat. Phys.* 12, 1100 (2016)) is purely theoretical, since its topological properties have not been observed directly in ARPES so far. Therefore, the fourfold degenerate Dirac nodal line in a real AFM material is still elusive. More importantly, in magnetic materials, band degeneracies usually lose the protection under SOC such as FM Fe_3GeTe_2 (*Nature Materials* 17, 794 (2018)) and FM Co_2MnGa (*Science* 365, 1278 (2019)). We rigorously verify the *gapless* AFM nodal line both theoretically through a detailed symmetry analysis, and experimentally by ARPES. Along with the Hund's coupling that closely interacts with the nodal line, this is a rare experimental band-resolved demonstration of topological nodal line phase under correlations.

Similarly, while Hund's coupling or strong correlations is not a novel concept and previous theoretical studies such as Ref 8 (*Phys. Rev. B* 83, 205101 (2011)) discuss topological phases under correlations, experimental band-resolved demonstration of such physics is still rare. We provide a solid experimental realization of the interplay of strong correlation and topology. Moreover, while the previous work (Ref 30) emphasizes a kondo-driven nontrivial topological phase due to the f orbitals, here in our work the correlation (Hund's coupling) is from Mn d orbitals. We also notice that recently there is an increasing interest in strong correlation and topology in various quantum materials including compounds with a pyrochlore lattice [R2 and R3].

[R2] Wakefield, J. P. et al. Three-dimensional flat bands in pyrochlore metal $CaNi_2$. *Nature* **623**, 301 (2023).
[R3] Huang, J. et al. Non-Fermi liquid behaviour in a correlated flat-band pyrochlore lattice. *Nat. Phys.* (2024).

iv) While the authors cite a somewhat random collection of more or less related topological states, a stronger focus on prior work in the area of electronic states in the presence of Hund coupling is recommended (e.g., Alonso et al., Phys. Rev. B 64, 054408, 2021). Specifically, referring to previous work on "Hund nodal lines," such as Geilhufe, Guinea, Juricic, Phys. Rev. B 99, 020404(R), 2019, would improve the manuscript's coherence.

We extend our sincere appreciation to the Referee for providing valuable references to enrich our work. We added relevant publications. Indeed they are closely related to our experimental results and should be acknowledged.

Reviewer #2 (Remarks to the Author):

The paper by Xian P. Yang et al. presents the electron structure of antiferromagnet YMn2Ge2 measured with ARPES. Compared with DFT and DMFT calculations, the authors suggest the fourfold degenerate Dirac nodal line states remain at the boundary of the bulk Brillouin zone ZRA plane, which is protected by PT symmetry and nonsymmetric

lattice symmetry. Furthermore, the authors compare the band d-orbital dependent renormalization factors from DFT, DMFT, and experiment results, and they claim that this Dirac nodal line is due to Hund's coupling so that this Dirac nodal line is a magnetic topological phase under electron correlations.

The paper is clear, and the findings are important for the topological and correlated matter community. I believe it's the first direct experiment result that observed the AFM Dirac nodal line states and the experiment measurements agree well with the theoretic band structures, which fill a gap in the magnetic topological materials.

We sincerely thank the Referee for the report and for clearly acknowledging the importance of our paper. We will respond to the questions and comments.

Apart from the advantages of this work, I have the following concerns and comments that need to be addressed prior to a recommendation for publication.

1. My main concern is that the bulk band crossing has not been fully proven to be bulk bands. On the contrary, they look more likely to be surface states in Fig. 2. I agree the Fermi surface mapping in Fig. 1c and Fig. 2a agree well with the DFT results, but the DFT results are dominated by surface states. How do the authors argue the crossing bands are bulk Dirac nodal states? In addition, in Fig. 4a, the DFT results show a crossing surface state close to the DP, so the pure surface states can also form the band shape in Fig. 1g. Extended Figs. 2 and 3 support the band along cut1 are bulk bands and they have crossing point along A-M, but the crossing points are very broad, which is hard to support the nodal line band structure. Additional evidence is necessary to prove the band along cut2 is a real bulk band crossing.

We thank the Referee for pointing this out. We would like to clarify that, while Fermi surface calculation in Fig. 1d has both surface and bulk contributions, our DFT results in Figs. 1f, h, j only have bulk bands. Therefore, based on a comparison between DFT and ARPES band dispersion, we believe the crossings are from the bulk Dirac nodal line. Additionally, even with VUV ARPES, we already observe a clear k_Z dependence of the nodal line (Supplementary Fig. 2), confirming the bulk sensitivity of the incident light.

The most straightforward and convincing evidence to confirm the bulk nature of a band dispersion is to perform soft X-ray ARPES. We thus demonstrate our bulk sensitive soft X-ray ARPES data on the nodal line. Based on photon energy dependence, photon energy of 552 eV corresponds to A-Z-R high symmetry plane. The Fermi surface map probed by 552 eV incident light is shown in Supplementary Fig. 3a. A line cut along A-R direction in Supplementary Fig. 3d clearly shows the nodal line feature in Fig. 1i (cut 3). The bulk band dispersion along Z-R direction is also demonstrated with the expected Dirac crossing at the R point (marked by the red arrow) in Supplementary Fig. 3b. The corresponding second curvature plot is shown to better resolve the crossing in Supplementary Fig. 3c. This is consistent with our VUV ARPES data in Fig. 1g (cut 2). Therefore, our new bulk sensitive ARPES data confirm the bulk origin of the Dirac cones and nodal line shown in Fig. 1.

We added the following to the main text: "Additionally, bulk sensitive soft X-ray ARPES also reveal the nodal line along A-R direction and the Dirac cone at R point (Supplementary Fig. 3), confirming their bulk origin."

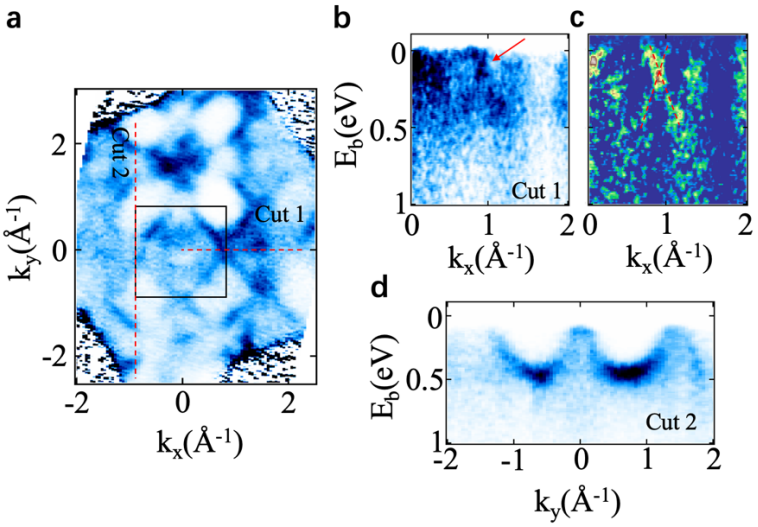

Supplementary Fig. 3. Soft X-ray ARPES on the AFM nodal line. a, ARPES Fermi surface spectrum on the (001) surface taken with incident photon energy of 552 eV corresponding to the A-Z-R high symmetry plane. The black box represents the Brillouin zone. Red dashed lines indicate the positions of cuts 1 and 2. **b,** ARPES dispersion along Z-R direction demonstrating the Dirac crossing at the R point (marked by the red arrow). **c,** Corresponding second curvature plot of **b**. Red dotted lines are a guide for the eye. **d,** ARPES dispersion along A-R direction demonstrating the Dirac nodal line. The bulk sensitive ARPES data confirm the bulk origin of the Dirac cone and the nodal line shown in Fig. 1.

Therefore, while there is a surface state close to the Dirac cone from DFT calculations in Fig. 4, it is not the band observed in ARPES. Another piece of evidence is that we can nicely trace the crossings along the nodal line in Fig. 2. These crossings are sharp and should clearly support the bulk nodal line band structure. Moreover, we demonstrate the crossing at the $\bar{M}$ point (or along A-M) to reveal the fourfold degeneracy at the other end of the nodal line in Supplementary Fig. 5. These points are expected to be much broader/incoherent, given that bulk bands at a deeper binding energy in a Hund metal should become more incoherent (for example, see DMFT calculations in Fig. 3).

2. How can we understand the drumhead surface states and why are the surface states split into two? Do they have different spin components? The authors should elaborate more on these drumhead surface states, e.g., are they different from non-magnetic Dirac nodal line drumhead surface states?

Thank you for giving us a chance to clarify this point. An easier way to understand the drumhead surface states is to consider two copies of Weyl crossings that move towards each other. A fermi arc is expected for each Weyl point. When these two twofold degenerate Weyl points move to the same momentum position, they can form a fourfold degenerate Dirac crossing with two surface states from the original two Weyl cones. Thus, the drumhead surface state in YMn_2Ge_2 splits into two branches. We also calculate the spin polarization of these surface states, and they indeed have interesting spin structures (Supplementary Fig. 11). Specifically, while there is negligible polarization in S_x and S_y directions, both drumhead branches show dominant spin polarization along the S_z direction, and they have *opposite* S_z spin. This could be verified by spin-resolved ARPES in the future.

Moreover, what sets AFM nodal line apart from nonmagnetic nodal line is its tunability. The AFM nodal line in YMn_2Ge_2 serves as a parent state leading to different topological phases including AFM Dirac semimetal, AFM Dirac nodal line and FM Weyl nodal surface (Supplementary Figs. 14-15). As a result, the corresponding drumhead surface state can be tuned with various magnetic phases.

We added a detailed discussion about drumhead states to the main text: "A simplified way to understand them is to consider two twofold degenerate Weyl points that move towards each other until they form a fourfold degenerate Dirac crossing. The two Fermi arc surface states from the original two Weyl cones could lead to the split drumhead surface states observed in ARPES, as further verified by the (001) surface constant energy contour calculations in Supplementary Fig. 10. Interestingly, these drumhead surface states show opposite spin polarization (Supplementary Fig. 11)." and "As a result, the corresponding drumhead surface state can be tuned with various magnetic phases."

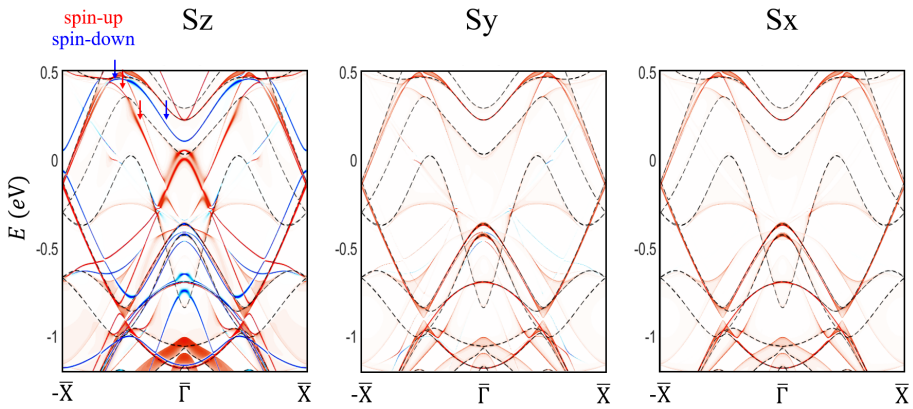

Supplementary Fig. 11. Spin polarization of the drumhead surface states. Spin polarization of the surface bands along the $\bar{X}$-$\bar{\Gamma}$-$\bar{X}$ high symmetry direction. The two drumhead surface states marked by the blue and red arrows display opposite S_z spin polarization and negligible polarization in S_x and S_y directions.

3. The bands maintain the fourfold degenerate along the M-A Brillouin boundary shown in Extended Figs. Are they also the Dirac nodal line?

Yes they are also Dirac nodal line. We have a detailed symmetry analysis in the methods section to illustrate the gapless nodal lines around the boundary of the whole 3D BZ (Supplementary Fig. 1). Therefore, there is also a nodal line along the A-M direction, in addition to the nodal line in the Z-R-A plane already shown in Figs. 1 and 2. To demonstrate this experimentally, we showed the $\bar{M}$-$\bar{\Gamma}$ cut at various k_z positions in Supplementary Figs. 5 a-f. For all the k_z positions we probed, two doubly degenerate bands cross to form a fourfold node (marked by the red arrows in Supplementary Figs. 5d-f) along the A-M line, thus confirming its fourfold degeneracy.

We also mention this in the main text: "We also trace the nodal line along the A-M direction. As shown by Supplementary Figs. 5**a-f,** the fourfold crossing at $\bar{M}$ point remains gapless along the k_z direction. Unlike the linear Dirac cone at the R point, the Dirac crossing at A point displays a parabolic dispersion (Supplementary Fig. 6)."

4. The band crossing along A-Z looks like parabolic lines. Could this crossing be proven as linear dispersion theoretically?

We thank the Referee for pointing this out. Our DFT calculations in Supplementary Fig. 6 below show that the band crossing at A point displays a parabolic dispersion. We added this figure as well as a short clarification in the main text: "Unlike the linear Dirac cone at the R point, the Dirac crossing at A point displays a parabolic dispersion (Supplementary Fig. 6)."

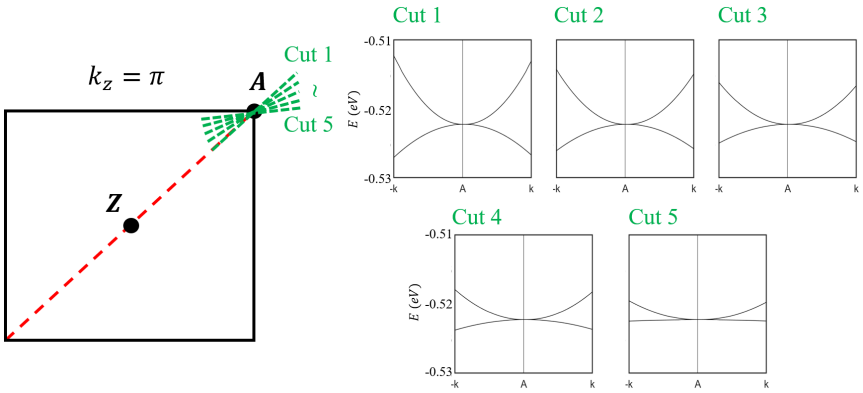

Supplementary Fig. 6. Quadratic band dispersions near the A point. Unlike the linear Dirac cone at R point, the Dirac crossing at A point displays a parabolic dispersion. Five cuts are extracted around A point, and all of them demonstrate a quadratic band crossing.

In addition to DFT calculations, the band dispersion from A to Z can be demonstrated theoretically. Since the bands along the boundaries of the BZ, such as A-R and A-M are fourfold degenerate, we need to construct a 4-band model, constrained by the symmetries preserved. At A point, the symmetries can be generated by $\tilde{\mathcal{T}}$, $\mathcal{P}$, $\widetilde{\mathcal{M}}_y$, and C_{4z}. Moreover, symmetries at A point satisfy the relationship $\{\mathcal{P}\tilde{\mathcal{T}}, \widetilde{\mathcal{M}}_i\} = 0$, $\{\widetilde{\mathcal{M}}_i, \widetilde{\mathcal{M}}_j\} = -2\delta_{ij}$, $\{\mathcal{P}, C_{4z}\} = 0$, $(\mathcal{P}\tilde{\mathcal{T}})^2 = -1$, and $\tilde{\mathcal{T}}^2 = 1$. Below we prove $\{\mathcal{P}, C_{4z}\} = 0$. For under the operations of $\mathcal{P}$ and C_{4z}, we have:

$$(x, y, z) \xrightarrow{C_{4z}} \left(-y + \frac{1}{2}, x, z\right) \xrightarrow{\mathcal{P}} \left(y - \frac{1}{2}, -x, -z\right)$$

$$(x, y, z) \xrightarrow{\mathcal{P}} (-x, -y, -z) \xrightarrow{C_{4z}} \left(y + \frac{1}{2}, -x, -z\right)$$

This indicates $C_{4z}\mathcal{P} = e^{-ik_y}\mathcal{P}C_{4z}$. As a result, $\mathcal{P}$ and C_{4z} satisfy anticommutation relation $\{\mathcal{P}, C_{4z}\} = 0$ at A point.

According to the four anticommutation relation at A point, we select the constraints of the symmetries at A point as $\mathcal{P}\tilde{\mathcal{T}} = \tau_1\sigma_2\mathcal{K}$, $\tilde{\mathcal{T}} = i\tau_2\sigma_2\mathcal{K}$, $\mathcal{P} = \tau_3$, $\widetilde{\mathcal{M}}_y = i\tau_3\sigma_2$, and $C_{4z} = \tau_1 \otimes e^{-i\frac{\pi}{4}\sigma_3}$. Consequently, the $k \cdot p$ low-energy effective model is constructed with three Γ -matrices, $\tau_3\sigma_{1,2,3}$, which can be expressed as

$$H_A(\vec{q}) = \alpha\left(q_x^2 + q_y^2\right)I_4 + \beta q_z^2 I_4 + \gamma q_x q_y \tau_3\sigma_3 + \lambda\left(q_z q_x \tau_3\sigma_2 - q_z q_y \tau_3\sigma_1\right)$$

Based on H_A, we find that the bands split into two doubly degenerate bands with parabolic dispersion when away from A point ($q_i = 0$).

For clarity, we have added the relevant descriptions to the revised manuscript.

5. The DFT results in Fig. 1d, f, h, j should be drawn in the same region as the experiment for better comparison.

We thank the Referee for the comment. We plot the DFT results in Fig. 1d on top of Fig. 1c for a better comparison. We will explain the comparison between ARPES results and Figs. 1f, h, j below.

One of our main conclusions in this study is that the magnetic nodal line in YMn_2Ge_2 is strongly renormalized due to Hund's coupling. As shown in Fig. 1j, A and R points consist of mostly d_{z^2} and d_{xy} orbitals, respectively. Therefore, distinct renormalization factors are needed for both *d* orbitals (or bands near A and R points), as an essential signature of a Hund's metal (Fig. 3). As a result, our globally renormalized DFT in Fig. 1 can only qualitatively catch the main features in the band structure, namely the energy position of the nodal point at R in Figs. 1g-h and the shape of the fourfold degenerate nodal line in Figs. 1i-j. At the same time, band dispersions at A point in DFT calculations deviate from ARPES data in Figs. 1e-f. The fact that DFT calculations don't fully agree with ARPES data near the Fermi level motivates us to apply DFT+DMFT to understand the band dispersion and electronic correlations. The important role Hund's coupling plays in this material is exactly the point we would like to emphasize in the manuscript.

To make it clearer to readers, we modify our text: "It is intriguing to note that to better match ARPES data, all bulk electronic bands in DFT calculations are renormalized by a factor of 3, suggesting the presence of strong electronic correlations in YMn_2Ge_2. Despite the overall good agreement especially the energy position of the nodal point at the R point in Figs. 1**g-j** and the shape of the nodal line in Figs. 1**i-j**, the binding energy position of the Dirac crossing at the A point differs from renormalized DFT calculations, as shown by the red dashed line in Figs. 1**e-f**. Instead, a smaller renormalization factor (less than 3) should be applied at the A point so that the bands are less "compressed" below the Fermi level. As we will show later, this magnetic nodal line manifests a strong *d* orbital dependent renormalization due to Hund's coupling. Therefore, DFT results in Fig. 1 don't fully agree with ARPES data, indicating the necessity of DFT + DMFT calculations that will improve the agreement (Supplementary Fig. 4 and Fig. 3)."

Furthermore, we add a new figure as Supplementary Fig. 4, which superimposes the DFT and the corresponding DFT+DMFT results on ARPES data (cuts 2 and 3 in Fig. 1) to highlight our argument. In Supplementary Fig. 4a, the Dirac dispersion in DFT matches well with ARPES data (black arrows), and the bulk band in ARPES near the Z point indicated by the blue arrows is also captured by DFT. The remaining two bands in ARPES near Z point are surface drumhead states (discussed in Fig. 4) so are not revealed in the bulk band DFT calculations. In the corresponding DFT+DMFT, these features remain, as demonstrated by black and blue arrows in Supplementary Fig. 4b. As a comparison, globally renormalized DFT cannot fully capture the band dispersion near the Fermi level along the A-R direction in Supplementary Fig. 4c, since the binding energy of the band near the A point in ARPES deviates from DFT calculations (marked by the black arrow). However, DFT+DMFT calculations with Hund's coupling included instead perfectly agree with ARPES (Supplementary Fig. 4d). Specifically, the dispersion near the A point is well captured by DFT+DMFT results.

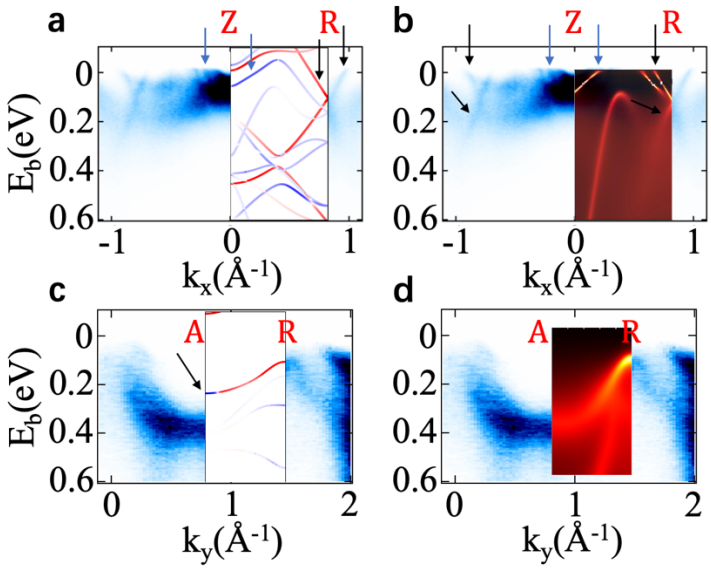

Supplementary Fig. 4. Comparison between ARPES and calculations. a, ARPES dispersion along Z-R direction. Same as Fig. 1**g** or cut 2 in Fig. 1. DFT calculations are superimposed on ARPES to illustrate the overall agreement. Blue and black arrows mark the bulk state at the center of the BZ and the Dirac cone, respectively. **b,** Same as **a,** except that DFT+DMFT results are superimposed on ARPES data. **c,** ARPES dispersion along A-R direction. Same as Fig. 1**i** or cut 3 in Fig. 1. The embedded DFT calculations deviate from ARPES data, especially near the A point (black arrow). **d,** Same as **c,** except that DFT+DMFT results are superimposed on ARPES data. The inclusion of Hund's coupling improves the agreement with ARPES.

For the comparison above, we only focus on band dispersions near the Fermi level, and we would like to explain the reason below. Given that YMn_2Ge_2 is a Hund metal, the broadening of the spectral function is a distinct feature of the strong correlations. Our DMFT spectral function in Fig. 3 shows the broadening of the spectral function at higher binding energies. For example, the sharp nodal line at R point becomes incoherent at A point. In APRES this Hund nodal line also reveals the same feature. Thus, bands at deeper binding energies are blurred/smeared out in experiments.

6. The axis region in Fig. 1i looks strange; the cut1 is -1 to 1, but the x-axis of Fig. 1i is 0 to 2, and the ARPES result in Fig. 1i looks like 0.5 to -1.5.

We thank the Referee for the careful proofreading. The axis region in Fig. 1i is correct since we extract the nodal line from the first BZ to the second BZ. Specifically, the marked point A is from the first BZ while the marked point R is from the sconed BZ. The dotted line for cut 3 in Fig. 1c was indeed kind of misleading, and we update it to better show the location of cut 3 in momentum space.

7. The region and high symmetry points of the 2nd Brillouin zone in Fig. 2a need to be added for clarity.

We thank the Referee for pointing this out. We marked the region and high symmetry points for the second BZ in Fig. 2a.

Reviewer #3 (Remarks to the Author):

The manuscript of X. P. Yang et. al. "A Hund nodal line antiferromagnet" reports Dirac nodal line along at the boundary of bulk Brillouin zone and a drumhead surface states through the whole surface Brillouin zone in YMn2Ge2 antiferromagnet. Electron correlation effects are unveiled.

The topic and material in general are interesting and important for the state of the art research. The nodal line looks confirmed, the results of the first manuscript half presented clear.

We sincerely thank the Referee for the comments and for clearly acknowledging the importance of our paper. We will address the concerns about the drumhead surface state below.

But with the drumhead surface state in this research there are problems. I do not see it on experimental data. The black dashed line at Fig. 4b goes differently from calculation at Fig. 4a. At Fig. 4a it initially coincides with the bulk state, at Fig. 4b goes initially apart from the bulk state.

Thanks for this important comment and affording us the opportunity to provide clarification on this matter. Given that YMn_2Ge_2 is a Hund metal, DFT alone without considering strong electronic correlation (Hund's coupling) cannot perfectly agree with ARPES band dispersion (DFT can only qualitatively catch the main features in the band structure). For example, band dispersions at A point in DFT calculations don't agree with ARPES data in Figs. 1e-f (or Supplementary Fig. 4). This explains why our ARPES data in Figs. 4b-c slightly deviates from the DFT calculations in Fig. 4a. Namely, in ARPES, the surface states move apart from the bulk state faster than DFT results. Additionally, the black dashed line in Fig. 4b is a guide for the eye. The extracted ARPES drumhead dispersion is shown as the black dots in Fig. 4c. It can be seen that the drumhead states are initially very close to the bulk state near the Dirac cone in Fig. 4c, and they move apart from the bulk state further away from the Dirac crossing. We update the black dashed line in Fig. 4b accordingly to better illustrate the experimental dispersion. Despite the slight difference between DFT and ARPES near the Dirac cone at the BZ boundary, calculations and experimental data match well around the center of the BZ. For example, the three electron pockets near the Fermi level at the BZ center are well reproduced in both Figs. 4a and 4b (marked by red and black arrows). Thus, DFT and ARPES overall are consistent.

Additionally, even in many *weakly* correlated topological materials, semi-infinite surface calculations usually are not perfectly consistent with ARPES results, due to various parameters that need to be adjusted/tuned in the complicated surface state DFT calculations. However, the nontrivial topology in YMn_2Ge_2, namely bulk Dirac nodal line and the corresponding drumhead surface state, is protected by the combination of magnetism, space-time inversion symmetry and nonsymmorphic lattice symmetry (more details about symmetry analysis are in methods section). DFT results indeed confirm the drumhead surface states that emerge from the bulk Dirac crossing. In other words, the main purpose of Fig. 4a is to demonstrate the topology of the material through DFT, which agree with ARPES data in Fig. 4b. In our study, the surface state emerges from the Dirac crossing both in ARPES data and DFT

calculations. In this sense, DFT sufficiently supports the bulk-boundary correspondence in YMn_2Ge_2, and leads to the conclusion that these surface states are indeed drumhead surface states.

In order to perfectly match the experimental surface band dispersion, DFT+DMFT surface calculation should be performed. However, this would require significantly intensive calculations given that bulk DFT+DMFT calculation in Fig. 3 is already quite hard. To the best of our knowledge, DFT+DMFT surface calculation has not been performed in correlated topological magnets due to the intensive workload required. Thus, we would leave this for a further work to study the nontrivial surface states in correlated topological magnets like YMn_2Ge_2 with DFT+DMFT calculations.

The surface state and bulk state do not coincide at the zone border at X at Fig. 4a.

Regarding the zone border at $\bar{X}$ point in Fig. 4a, we would like to clarify that the surface state (red arrows in Fig. R1 below) and bulk state do cross at the same point, as this is guaranteed through the bulk-boundary correspondence of the nodal line structure. The Referee might be confused by another surface state near the Dirac cone, as marked by the black arrow in the figure below. This surface state has nothing to do with topology and is a normal surface state.

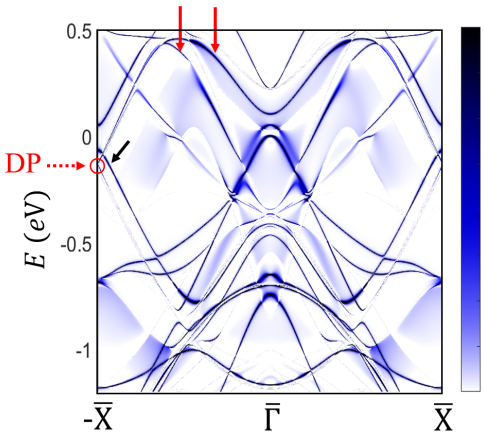

Fig. R1. ARPES dispersion along the $\bar{X}$-$\bar{\Gamma}$-$\bar{X}$ high symmetry direction. Red solid arrows represent the drumhead surface state, while the black arrow denotes another surface state not associated with the nodal line. Red dash line pointing to the red circle marks the bulk Dirac cone.

Extended Fig. 5 shows a different picture inside the zoom-in green box compared to the left panel.

We thank the Referee for the careful proofreading. We realized that the size of the zoom-in green box was wrong in the original version. We updated it with the correct size and location. In the new version, the zoom-in view is consistent with the overall calculations. Moreover, it clearly shows that the drumhead surface states and the bulk Dirac cone coincide at $\bar{X}$ point. We also attach the updated Supplementary Fig. 8 below.

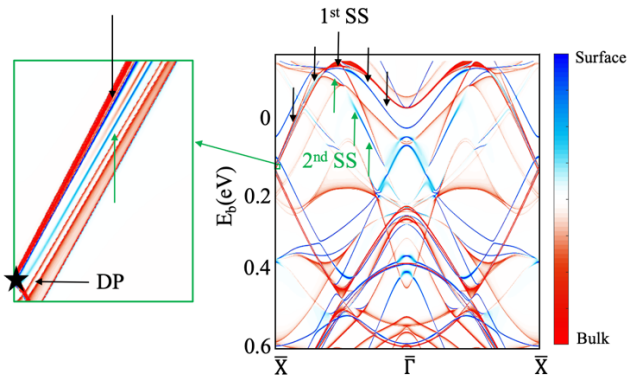

Supplementary Fig. 8. Drumhead surface state in YMn_2Ge_2. Semi-infinite surface calculations along the $\bar{X}$-$\bar{\Gamma}$-$\bar{X}$ high symmetry direction. Color bar indicates the surface state contribution. Black and green arrows mark the positions of the two drumhead surface states from the Dirac crossing. The left zoom in plot corresponds to the green box at the Dirac crossing. Black star represents the location of the Dirac point. Two surface states marked by the black and green arrows emerge from the bulk Dirac node.

I expect also that the drumhead surface state should be visible at Fig. 2, but it is not visible. Why?

We thank the Referee for the comment. In Fig. 2 we want to emphasize the bulk nodal line dispersion clearly. Thus, we choose to show the ARPES dispersions in the second Brillouin zone. Accordingly, Fig. 2a is the Fermi surface in the second Brillouin zone. Due to matrix element effect, only the bulk bands are clearly observed in the second Brillouin zone. Fig. 4b, on the other hand, is taken in the first Brillouin zone. We clarify this point in the main text: "To highlight the bulk nodal line dispersions clearly, we choose to show the second BZ in Fig. 2, since the surface states near the bulk bands are suppressed due to matrix element effect compared with the first BZ."

Moreover, Supplementary Fig. 9 shows photon energy dependence of the drumhead states at five photon energies (or kz positions). Both MDC and EDC curves clearly confirm that drumhead states have a surface nature, since they don't vary with photon energies. As a comparison, the bulk state (marked by the red arrow) changes with different photon energies given its bulk origin.

The calculation of Fig. 4a shows a huge number of surface bands. By which criteria some of the bands are considered and others neglected in the discussion? With such number of calculated surface bands one can find anything and a faint band on one of the measurements (but not others) can be attributed also to anything.

As the result, an important part of the manuscript is unconfirmed within the current presentation and can not be published in the present form.

Thanks for this important question and the opportunity for giving us a chance to clarify this point. The two drumhead surface states differ from other surface bands due to the bulk-boundary correspondence. Namely, unlike other states, drumhead surface states are expected to emerge from the bulk nodal line. From our DFT results in Supplementary Fig. 8, we can clearly see the two drumhead surface states that are connected with the bulk Dirac cone. Supplementary Fig. 10 below also reveals these surface states on (001) termination constant energy contour. Specifically, only the drumhead states emerge from the bulk Dirac crossing in the zoom-in plot of Supplementary

Fig. 10b. Moreover, these two states display a dominant spin polarization along the z direction. Interestingly, the spin polarization is opposite (Supplementary Fig. 11). Thus, while there are several surface states near the Dirac crossing, our theoretical calculations clearly establish the existence of two drumhead surface bands. Our experimental data also demonstrate a reasonable agreement with DFT results in Fig. 4.

We thereby added the relevant discussion about drumhead states to the main text: "… as further verified by the (001) surface constant energy contour calculations in Supplementary Fig. 10. Interestingly, these drumhead surface states show opposite spin polarization (Supplementary Fig. 11)."

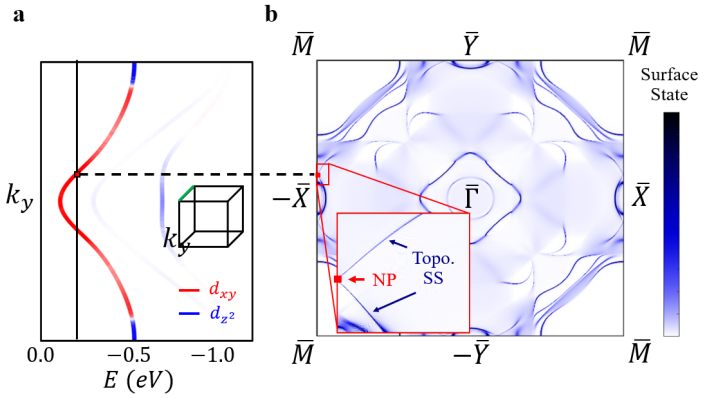

Supplementary Fig. 10. Drumhead surface state on the (001) surface. a, Dirac nodal line along the A-R direction. Same as Fig. 1**j**. Black vertical line denotes the binding energy of the constant energy contour in **b**. **b,** Constant energy contour integrated over all the k_z values on the (001) surface. The zoom-in plot displays the location of the Dirac crossing and the corresponding two drumhead surface states emerging from it.

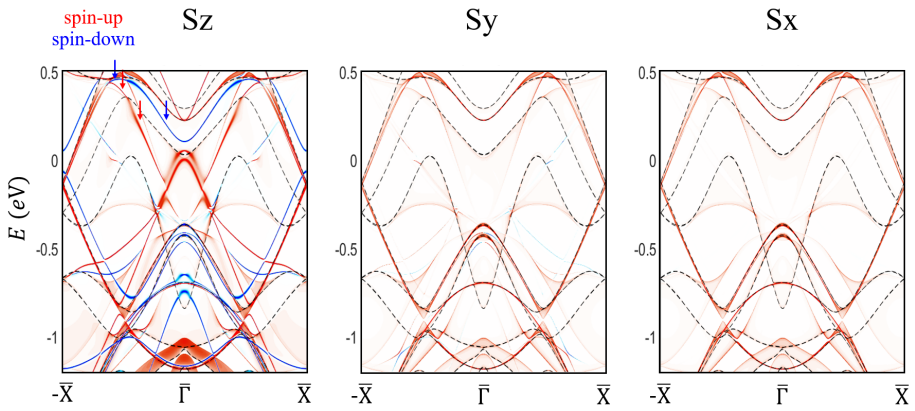

Supplementary Fig. 11. Spin polarization of the drumhead surface states. Spin polarization of the surface bands along the $\bar{X}$-$\bar{\Gamma}$-$\bar{X}$ high symmetry direction. The two drumhead surface states marked by the blue and red arrows display opposite S_z spin polarization and negligible polarization in S_x and S_y directions.

We thank all the Referees again for their time and valuable suggestions. We have carefully addressed all comments and suggestions. We hope now that the manuscript meets the high standard of Nature Communications.

REVIEWER COMMENTS

Reviewer #1 (Remarks to the Author):

The authors have substantially revised their manuscript and addressed the referees' concerns. Although the agreement between experiment and ab initio calculations remains loose, important features persist, and the authors have improved their figures to highlight these features. The supplementary Figure 13, which shows the densities throughout the bulk, is excellent and demonstrates the topological nature of the line node. Given the challenge in material identification and experimentation, along with the positive feedback from the other referees, I recommend the manuscript for publication in Nature Communications.

Reviewer #2 (Remarks to the Author):

The authors have carefully considered all comments from the reviewers and have updated their manuscript accordingly. The manuscript is much improved and the additional supplemental figures help solidify the author's arguments and conclusions. I recommend the manuscript for publication in its current form.

Reviewer #3 (Remarks to the Author):

See attached file.

1) The raised questions are partially answered. It is probable that the authors are right with their interpretation of the drumhead surface states, however I do not see it being proved clearly. There are some moments which are on the level of interpretation, but one could imagine other interpretations. As an example, on figure below I can trace the surface state band dispersion (see the circle region) differently from authors and this will change a lot of things in the manuscript.

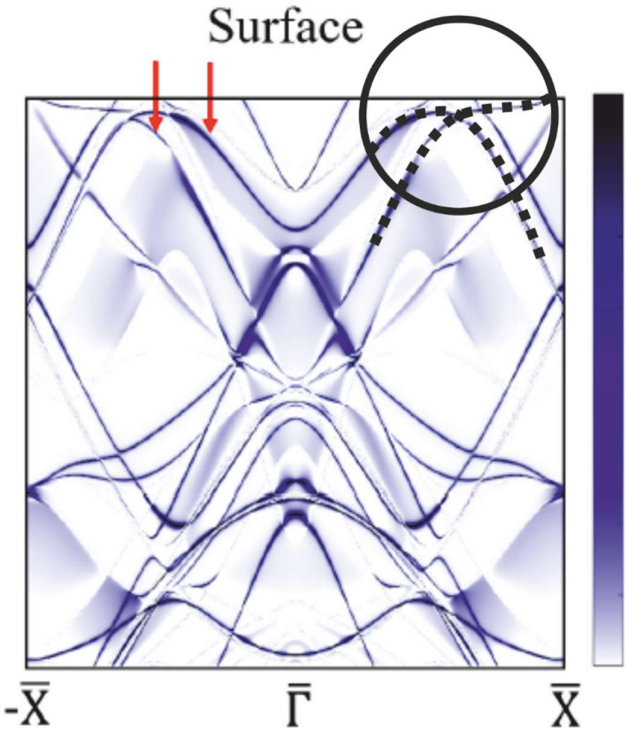

2) I suppose that not any nodal line must have drumhead surface state. Can authors provide more information on the expectation that in the current case it must be present?

3) A minor question: The Brillouin zone is shown always as cubic in the manuscript (for simplicity?). This can be misleading.

4) The figure below shows how the drumhead surface state goes from the Dirac point upwards together with the bulk bands. There is also a 'normal' surface state at the bottom part which does not go to the DP. However, one can see a blue line (surface state) from the DP downwards. This state is nearly hidden behind the red bulk band line. Because it starts from the DP and goes along the bulk band, should it be also a drumhead surface state? What is the difference and how could you distinguish the drumhead SS from the normal one?

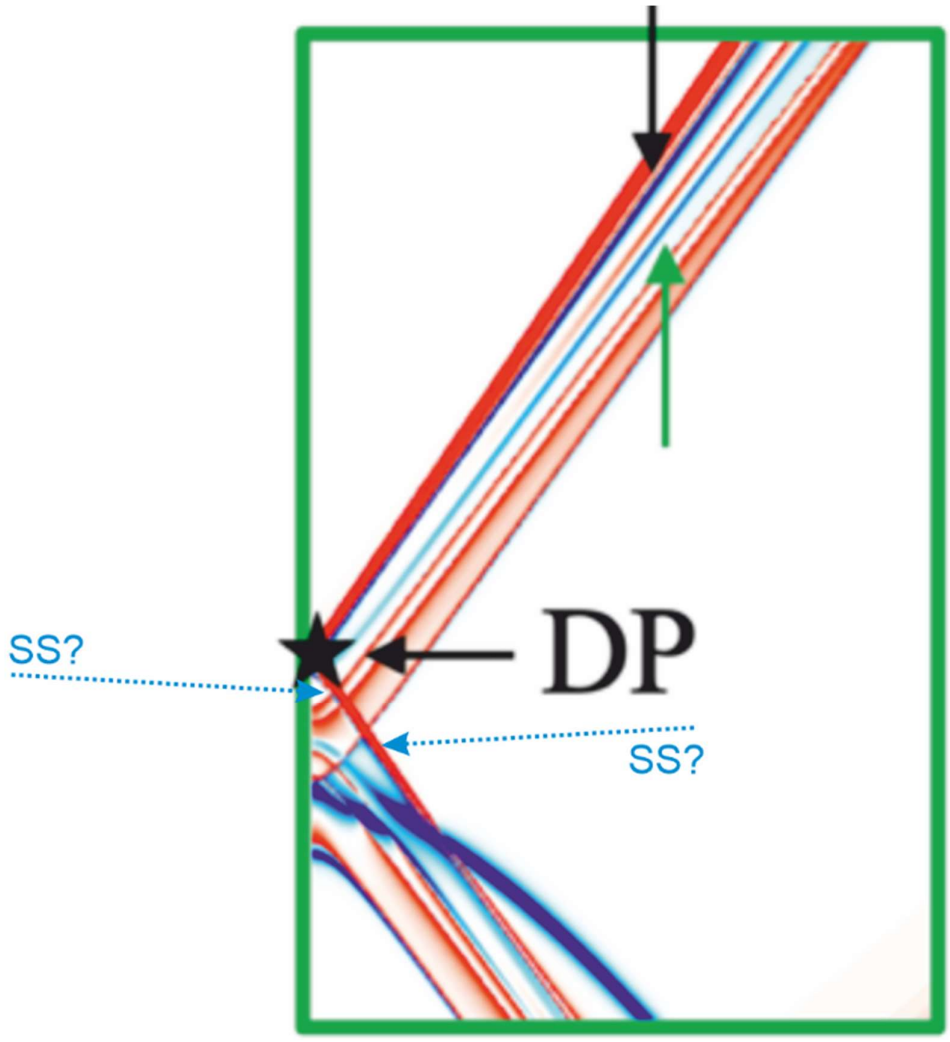

As the conclusion, I see the work interesting but not all of the results proved unambiguously. At least one more round of revision is needed.

Authors' Reply to Referees' Comments

We wish to thank all Referees for their insightful comments and suggestions, which greatly helped improve our manuscript. In the following, we carefully address their comments.

Reviewer #1:

The authors have substantially revised their manuscript and addressed the referees' concerns. Although the agreement between experiment and ab initio calculations remains loose, important features persist, and the authors have improved their figures to highlight these features. The supplementary Figure 13, which shows the densities throughout the bulk, is excellent and demonstrates the topological nature of the line node. Given the challenge in material identification and experimentation, along with the positive feedback from the other referees, I recommend the manuscript for publication in Nature Communications.

We would like to sincerely thank the Referee for the detailed comments and questions, and we are excited to hear that the Referee agrees for publication.

Reviewer #2:

The authors have carefully considered all comments from the reviewers and have updated their manuscript accordingly. The manuscript is much improved and the additional supplemental figures help solidify the author's arguments and conclusions. I recommend the manuscript for publication in its current form.

We extend our sincere appreciation to the Referee for providing valuable insights to enrich our work, and we are thrilled to know that the Referee now recommends our work for publication.

Reviewer #3:

1. The raised questions are partially answered. It is probable that the authors are right with their interpretation of the drumhead surface states, however I do not see it being proved clearly. There are some moments which are on the level of interpretation, but one could imagine other interpretations. As an example, on figure below I can trace the surface state band dispersion (see the circle region) differently from authors and this will change a lot of things in the manuscript.

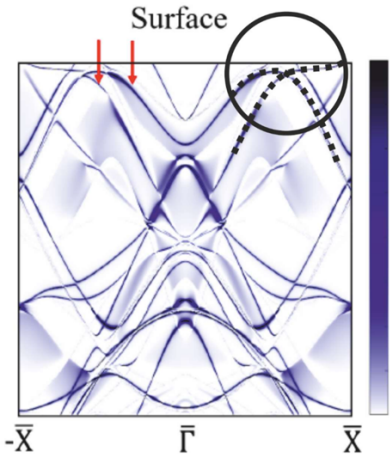

Thank you for giving us a chance to clarify this point. While it seems that the second drumhead surface state might not be connected to the bulk Dirac cone like the Referee suggests, we provide a zoom-in plot below to exclude this possibility. As indicated by the black circle in Fig. R1 below, the surface states (marked by black arrows) proposed by the Referee are not connected, so these two surface states belong to separate surface dispersions. As a result, our identification of drumhead states should be valid.

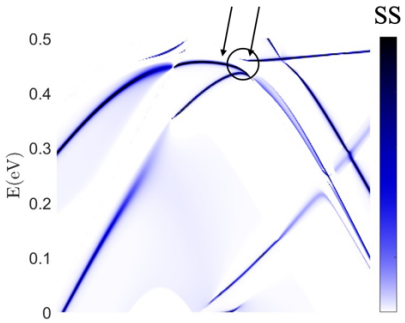

Fig. R1. Zoom in plot of the drumhead states in YMn_2Ge_2. Zoom in plot of semi-infinite surface calculations along the $\bar{X}$-$\bar{\Gamma}$-$\bar{X}$ high symmetry direction.

2. I suppose that not any nodal line must have drumhead surface state. Can authors provide more information on the expectation that in the current case it must be present?

We thank the Referee for the comment. As we explained to the second Referee in our previous reply, a simpler way to understand the drumhead surface states in YMn_2Ge_2 is to consider two copies of Weyl crossings that move towards each other. Since the topologically protected Fermi arc surface state connects the projections of Weyl points on the surface BZ, a fermi arc is expected for each Weyl node. When two twofold degenerate Weyl points move to the same momentum position, they can form a fourfold degenerate Dirac crossing with two surface states from the original two Weyl cones. Thus, there are two drumhead surface states in YMn_2Ge_2 that split into two branches. Indeed, our DFT calculations confirm the two drumhead surface states emerging from the bulk Dirac cone in YMn_2Ge_2 (for example in Supplementary Figs. 8 and 10),

demonstrating the bulk-boundary correspondence of the Dirac nodal line. Thus, in YMn_2Ge_2 the drumhead surface states are expected.

Additionally, we provide another piece of evidence to illustrate why drumhead surface states are expected in YMn_2Ge_2 from a theoretical point of view. The drumhead surface state in a nodal line semimetal is generally protected by a quantized π Zak phase, which represents the Berry phase of a straight line normal to the surface and crossing the bulk Brillouin zone (BZ) [R1]. Supplementary Fig. 16 below illustrates the Zak phase $\mathcal{Z}(k_x, k_y)$ along the k_z axis in the bulk BZ, perpendicular to the (001) plane, by using Wilson loop, similar to a previous paper [R1]. Our calculations show that the Zak phase at point **a** is quantized to $-\pi$, denoted as $\mathcal{Z}(\mathbf{a}) = -\pi$ (Supplementary Fig. 16a). The Zak phase remains constant until the line intersects the nodal line. Due to symmetries, the Dirac nodal line in YMn_2Ge_2 is constrained to lie on the BZ boundary (blue lines), resulting in a quantized Zak phase $\mathcal{Z}(k_x, k_y) = -\pi$ at any point on the $k_x - k_y$ plane, as shown in Supplementary Figs. 16 b-d. When the line crosses the Dirac nodal line at the BZ boundary, the Zak phase changes by 2π, corresponding to the Berry phase of the Dirac nodal line. Consequently, the Zak phase $\mathcal{Z}(k_x, k_y) = -\pi$ for any gapped state leading to the formation of drumhead surface states on the (001) surface. Therefore, the appearance of drumhead states in YMn_2Ge_2 is dictated by the bulk nodal line structure, and thus should be expected.

[R1] Li, X.-P. et al. Double Dirac nodal line semimetal with a torus surface state. *Phys. Rev. B* **103**, L161109 (2021).

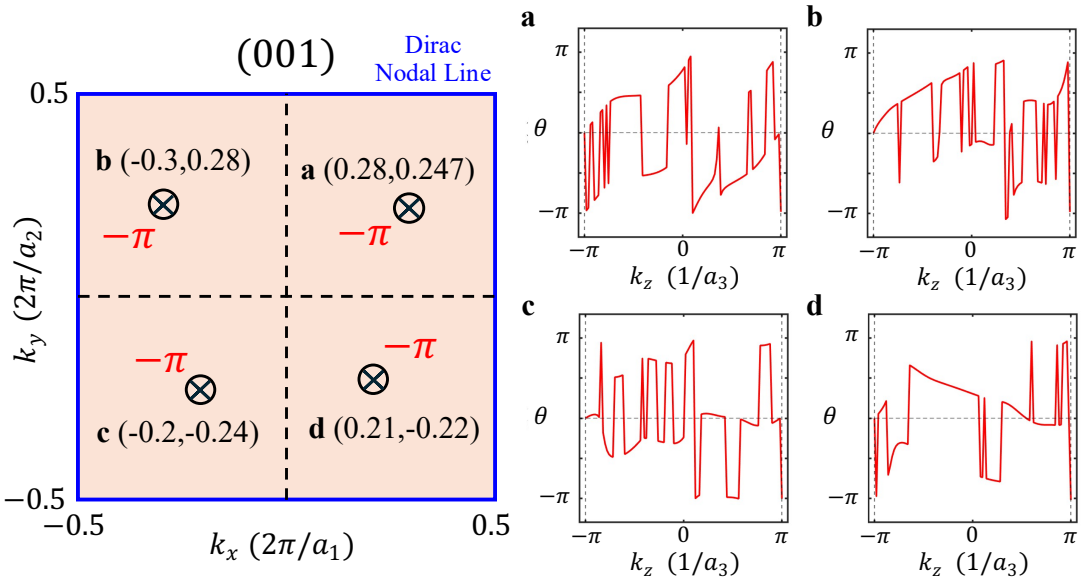

Supplementary Fig. 16. Schematic figure of the Zak phase by integrating k_z axis corresponding to (001) surface states. a-d, Wilson Loop along k_z axis for a-d points

marked in the left panel. Since the Zak phase $\mathcal{Z}(k_x, k_y) = -\pi$ for any point on the $k_x - k_y$ plane, drumhead surface states are expected on the (001) surface in YMn_2Ge_2.

We added Supplementary Fig. 16 accordingly. We also updated the short discussion about the drumhead states in the main text: "A simplified way to understand them is to consider two twofold degenerate Weyl points that move towards each other until they form a fourfold degenerate Dirac crossing. Since a fermi arc is expected for each Weyl node, the two Fermi arc surface states from the original two Weyl cones could lead to the split drumhead surface states observed in ARPES, as further verified by the (001) surface constant energy contour calculations in Supplementary Fig. 10."

Moreover, we added a new part in the Method section related to Supplementary Fig. 16: "**Zak phase of the drumhead surface states.** We provide a theoretical point of view to illustrate why drumhead surface states are expected in YMn_2Ge_2. The drumhead surface state in a nodal line semimetal is generally protected by a quantized π Zak phase, which represents the Berry phase of a straight line normal to the surface and crossing the bulk BZ [64]. Supplementary Fig. 16 shows the Zak phase $\mathcal{Z}(k_x, k_y)$ along the k_z axis in the bulk BZ, perpendicular to the (001) plane, by using Wilson loop [64]. Our calculations demonstrate that the Zak phase at point **a** is quantized to $-\pi$, denoted as $\mathcal{Z}(\mathbf{a}) = -\pi$ (Supplementary Fig. 16**a**). The Zak phase remains constant until the line intersects the nodal line. Due to symmetries, the Dirac nodal line in YMn_2Ge_2 is constrained to lie on the BZ boundary (blue lines), resulting in a quantized Zak phase $\mathcal{Z}(k_x, k_y) = -\pi$ at any point on the $k_x - k_y$ plane, as shown in Supplementary Figs. 16**b-d**. When the line crosses the Dirac nodal line at the BZ boundary, the Zak phase changes by 2π, corresponding to the Berry phase of the Dirac nodal line. Consequently, the Zak phase $\mathcal{Z}(k_x, k_y) = -\pi$ for any gapped state leading to the formation of drumhead surface states on the (001) surface. Therefore, the appearance of drumhead states in YMn_2Ge_2 is protected by the bulk nodal line structure, and thus should be expected."

3. A minor question: The Brillouin zone is shown always as cubic in the manuscript (for simplicity?). This can be misleading.

We thank the Referee for the careful proofreading. The Brillouin zone was cubic in the main text for simplicity. We have updated the Brillouin zone shape based on the crystal lattice constants (c is longer than a and b). We also attached the updated figures below.

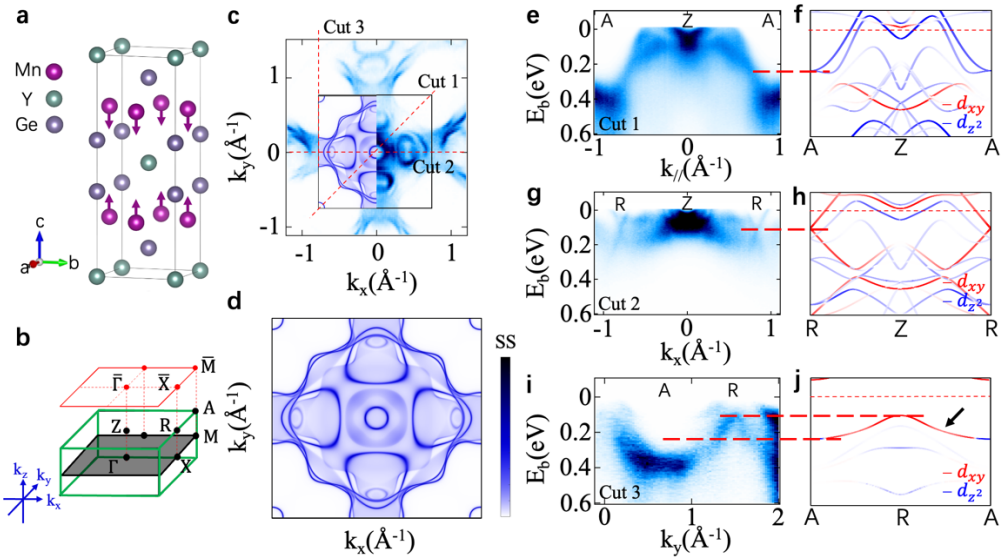

Fig. 1. Fermi surface and AFM Dirac line in YMn_2Ge_2. a, The crystal structure of YMn_2Ge_2. The purple arrows indicate that the two adjacent ferromagnetic Mn layers have opposite spin directions. **b**, Bulk and surface Brillouin zones (BZs) of YMn_2Ge_2. High symmetry points are marked. The magnetic nodal line around the boundary of the BZ is highlighted by the green line. **c**, ARPES Fermi surface spectrum on the (001) surface. The black square represents the surface BZ. Red dashed lines indicate ARPES dispersion cuts 1-3 in **e-j**. **d,** Calculated Fermi surface map corresponding to the black box in **c** and integrated over all the k_z values. The same plot is also embedded in **c**. **e-f,** ARPES dispersion map (**e**) and the corresponding bulk band structure calculation (**f**) along cut 1 in **c**. High symmetry points are marked. Mn d_{z^2} (blue) and d_{xy} (red) orbitals are projected on the bulk bands. The Fermi level in **f** is adjusted according to the experimental data and DFT is renormalized by 3. Two doubly degenerate bands cross at the A point to form a fourfold degeneracy. Thick red dashed line shows that the binding energy of the Dirac crossing at the A point in the renormalized DFT differs from experimental data. **g-h,** ARPES dispersion map (**g**) and the corresponding bulk band structure calculation (**h**) along cut 2 in **c**. A fourfold Dirac crossing can be seen at the R point. The thick red dashed line shows the consistency between the renormalized DFT and experimental data especially at the R point. **i-j,** ARPES dispersion map (**i**) and the corresponding bulk band structure calculation (**j**) along cut 3 in **c**. Thick red dashed lines suggest that although the renormalized DFT correctly describes the band dispersion near the R point, it doesn't agree well with ARPES data at the A point. Black arrow in **j** indicates the nodal line, and A and R points consist of mostly d_{z^2} and d_{xy} orbitals, respectively.

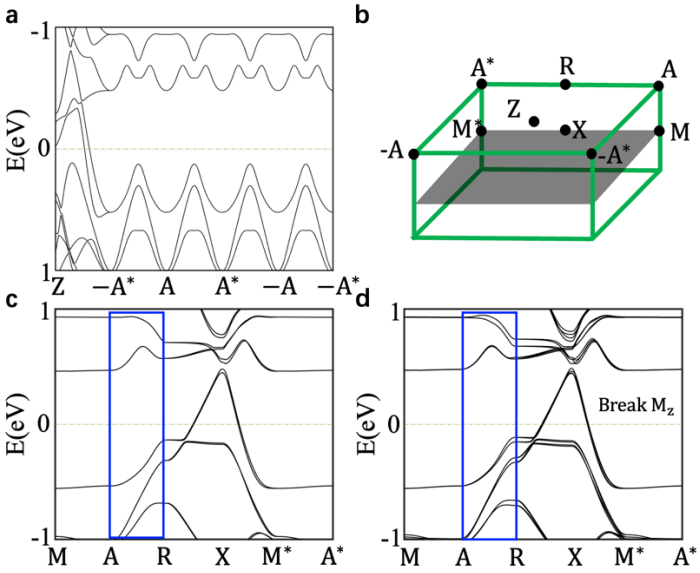

Supplementary Fig. 1. Calculated bulk electronic band structure along the boundary of the Brillouin zone with spin-orbit coupling and magnetism included. **a,** DFT calculations of the fourfold degenerate AFM nodal line on the Z-R-A plane. The nodal line forms a closed loop along the boundary of the Brillouin zone (BZ) on the Z-R-A plane. **b,** Bulk BZ of YMn_2Ge_2 with high symmetry points marked. The magnetic nodal line around the boundary of the 3D BZ is indicated by the green lines. **c,** DFT calculations of the fourfold nodal line on the M-A-X-R high symmetry plane. Fourfold bands exist only along the boundary of the BZ, consistent with our symmetry analysis. **d,** If M_z mirror symmetry is broken, the fourfold nodal line would split into two branches, highlighted by the blue rectangle. This demonstrates how mirror symmetry protects the AFM nodal line.

4. The figure below shows how the drumhead surface state goes from the Dirac point upwards together with the bulk bands. There is also a 'normal' surface state at the bottom part which does not go to the DP. However, one can see a blue line (surface state) from the DP downwards. This state is nearly hidden behind the red bulk band line. Because it starts from the DP and goes along the bulk band, should it be also a drumhead surface state? What is the difference and how could you distinguish the drumhead SS from the normal one?

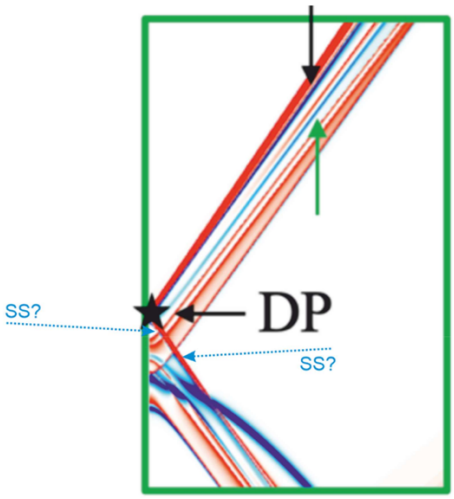

We thank the Referee for the comment. To reveal the drumhead surface states emerging from the bulk Dirac cone in YMn_2Ge_2, we provide relevant DFT calculations in Supplementary Figs. 8 and 10. In Supplementary Fig. 8, as suggested by the Referee, there is a third surface state that is very close to the bulk Dirac cone, making it tricky to distinguish from the two drumhead surface states both identified in DFT and ARPES data. To better distinguish them, we provide a zoom-in plot in Supplementary Fig. 10b, which clearly displays the bulk Dirac cone as well as the corresponding two drumhead surface states, without the third surface state marked by the Referee. This suggests that only the two drumhead surface states are directly linked with the Dirac cone. Therefore, Supplementary Figs. 8 and 10 as a whole reveal the bulk-boundary correspondence in YMn_2Ge_2.

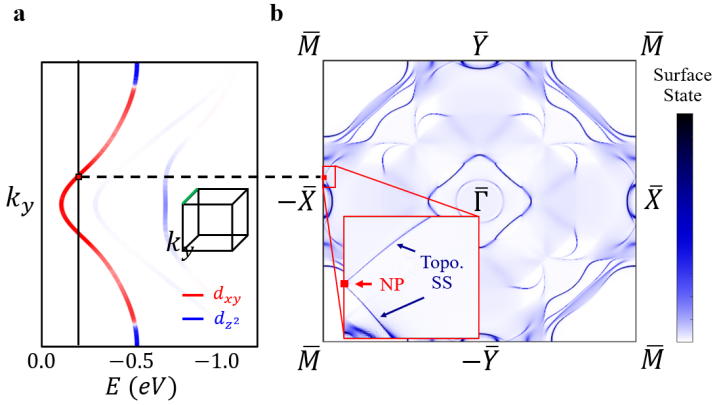

Supplementary Fig. 10. Drumhead surface state on the (001) surface. a, Dirac nodal line along the A-R direction. Same as Fig. 1**j**. Black vertical line denotes the binding energy of the constant energy contour in **b**. **b,** Constant energy contour integrated over all the k_z values on the (001) surface. The zoom-in plot displays the location of the Dirac crossing and the corresponding two drumhead surface states emerging from it.

Apart from DFT calculations, we also provide another perspective to illustrate why drumhead surface states are expected to exist in YMn_2Ge_2. Like we already explained in our reply to the second question, since the Zak phase $\mathcal{Z}(k_x, k_y) = -\pi$ for any point on the $k_x - k_y$ plane, drumhead surface states are expected on the (001) surface in YMn_2Ge_2. In Supplementary Fig. 16, when the line crosses the Dirac nodal line at the BZ boundary, the Zak phase changes by 2π, corresponding to the Berry phase of the Dirac nodal line. Therefore, the appearance of drumhead states in YMn_2Ge_2 is dictated by the bulk nodal line structure, and thus should be expected. As a comparison, the normal surface state, as pointed out by the Referee, doesn't represent the topology of the bulk nodal line, even if it is very close to the Dirac cone.

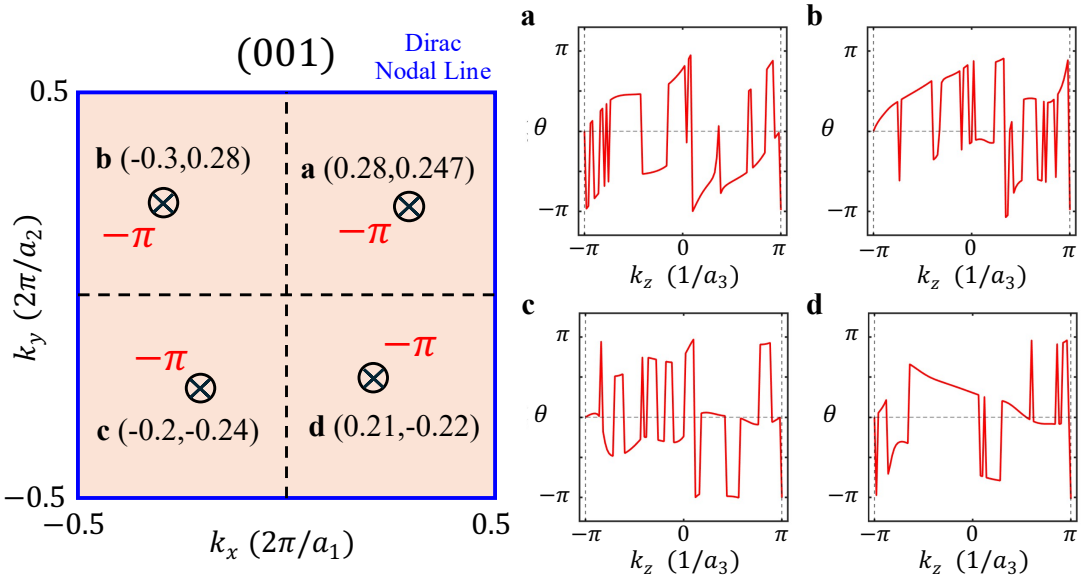

Supplementary Fig. 16. Schematic figure of the Zak phase by integrating k_z axis corresponding to (001) surface states. a-d, Wilson Loop along k_z axis for a-d points marked in the left panel. Since the Zak phase $\mathcal{Z}(k_x, k_y) = -\pi$ for any point on the $k_x - k_y$ plane, drumhead surface states are expected on the (001) surface in YMn_2Ge_2.

As the conclusion, I see the work interesting but not all of the results proved unambiguously. At least one more round of revision is needed.

We updated our main text and figures based on Referee's comments and we hope now we have unambiguously established the existence of drumhead surface states both theoretically and experimentally.

We thank all the Referees again for their time and valuable suggestions. We have carefully addressed all comments and suggestions. We hope now that the manuscript meets the high standard of Nature Communications.